



## MUNIN: Application of three-way decomposition to the analysis of heteronuclear NMR relaxation data\*\*

Dmitry M. Korzhnev<sup>a,b</sup>, Ilghiz V. Ibraghimov<sup>c</sup>, Martin Billeter<sup>a,d</sup> & Vladislav Yu. Orekhov<sup>a,\*</sup>

<sup>a</sup>Swedish NMR Centre at Göteborg University, Box 465, 40530 Göteborg, Sweden

<sup>b</sup>Shemyakin-Ovchinnikov Institute of Bioorganic Chemistry, Russian Academy of Sciences, ul. Miklukho-Maklaya 16/10, 117997 Moscow, Russia

<sup>c</sup>Saarbrücken University, Mathematical Department, Saarbrücken, D-66041, Germany

<sup>d</sup>Göteborg University, Lundberg Laboratory, Biochemistry and Biophysics, Box 462, 40530 Göteborg, Sweden

Received 18 June 2001; Accepted 24 August 2001

**Key words:** canonical decomposition, dynamics, parallel factor analysis, proteins, relaxation, rotating frame, three-way decomposition

### Abstract

MUNIN (Multidimensional NMR Spectra Interpretation), a recently introduced approach exploiting the mathematical concept of *three-way decomposition*, is proposed for separation and quantitative relaxation measurements of strongly overlapped resonances in sets of heteronuclear two-dimensional spectra that result from typical relaxation experiments. The approach is general and may also be applied to sets of two-dimensional spectra with arbitrary modulation along the third dimension (e.g., J-coupling, diffusion). Here, the method is applied for the analysis of <sup>15</sup>N rotating frame relaxation data.

Heteronuclear NMR relaxation measurements provide a versatile tool for studying protein structure and dynamics (Korzhnev et al. 2001; Palmer et al., 1996). Numerous relaxation experiments on <sup>15</sup>N, <sup>13</sup>C and <sup>2</sup>H nuclei allow detailed descriptions of protein motions occurring in time-scales from picoseconds to hours (Kay, 1998), while structural information can be gained from cross-correlated relaxation measurements (Kumar et al., 2000). A typical output of a relaxation experiment consists of a set of <sup>15</sup>N- or <sup>13</sup>C-edited two-dimensional spectra recorded with different conditions for the relaxation of the coherence studied. The property of interest (e.g., relaxation rate) is extracted from peak intensities. Spectral overlap of resonances can significantly complicate the analysis to the extent that relaxation data for overlapped peaks are often disregarded or interpreted only qualitatively. Experiments that remove the overlap typically require

extended measurement times as well as <sup>13</sup>C labeling, an example being the suite of HNC0 based three-dimensional experiments designed for backbone <sup>15</sup>N relaxation measurements in <sup>15</sup>N/<sup>13</sup>C labeled proteins (Caffrey et al., 1998). The present communication describes a method allowing quantitative relaxation measurements for strongly overlapped resonances using an ordinary set of two-dimensional spectra obtained in relaxation experiments (e.g., for <sup>15</sup>N  $R_1$ ,  $R_2$  or  $R_{1\rho}$ ). A set of <sup>1</sup>H-<sup>15</sup>N correlation spectra comprising <sup>15</sup>N  $R_{1\rho}$  data for the 14 kDa protein azurin (Karlsson et al., 1989) is analyzed using the MUNIN (Multidimensional NMR Spectra Interpretation) approach (Orekhov et al., 2001), which exploits the mathematical concept of *three-way decomposition* (Bro, 1997). While a compilation of the complete set of <sup>15</sup>N  $R_{1\rho}$  relaxation data for azurin will be presented and discussed elsewhere, we illustrate here the capabilities of MUNIN using strongly overlapped spectral regions in sets of as few as 11 two-dimensional spectra.

\*To whom correspondence should be addressed. E-mail: orov@nmr.se

\*\*MUNIN software is available from the authors.

Off-resonance  $R_{1\rho}$  measurements for the azurin backbone  $^{15}\text{N}$  nuclei were carried out on an 18.8 T Varian *Inova* spectrometer using a pulse-sequence described by (Mulder et al., 1998). Spectra were acquired at 15 °C for a 1 mM sample of uniformly  $^{15}\text{N}$  labeled reduced protein dissolved in potassium phosphate buffer at pH 5. The alignment of  $^{15}\text{N}$  magnetization along the effective field was performed by a 6 ms  $\tanh/\tan$  adiabatic pulse. The spin-lock field strength was  $1410 \pm 35$  Hz. The experiment was performed with 19 offsets of the  $^{15}\text{N}$  spin-lock field ranging from  $-7000$  to  $7000$  Hz from the center of the spectrum. Eleven spectra were recorded for each offset with spin-lock lengths ranging from 0 to 250 ms. Spectral widths of 10 and 3 kHz, and acquisition times of 99 and 40 ms were used in  $^1\text{H}$  and  $^{15}\text{N}$  dimensions respectively. Thus, the measured data set comprises 209 two-dimensional  $^1\text{H}$ - $^{15}\text{N}$  spectra. All spectra were zero-filled to  $8\text{k} \times 4\text{k}$  complex points prior to Fourier transform. Gaussian and sine-bell weighting functions were applied along the  $^1\text{H}$  and  $^{15}\text{N}$  dimensions, respectively.

A set of two-dimensional spectra obtained in relaxation experiments can be considered as a pseudo three-dimensional data matrix with the third dimension corresponding to the evolution due to relaxation of the coherence studied. Thus, the data consists of an  $I \times J \times K$  array with  $I$ ,  $J$  and  $K$  number of points in proton, heteronuclear and ‘relaxation’ dimensions, respectively. In the frame of the MUNIN approach this array is approximated by a sum of  $N$  rank-one tensors (components), each given by the direct product of three one-dimensional shapes:

$$S_{i,j,k} = \sum_{m=1}^N A_m^m F_1^m F_2^m F_3^m + e_{i,j,k}. \quad (1)$$

Here,  $S_{i,j,k}$  and  $e_{i,j,k}$  ( $i=1\dots I$ ,  $j=1\dots J$ ,  $k=1\dots K$ ) are matrix elements describing the experimental three-dimensional data set and residuals, respectively. Each of the  $N$  components represents a particular resonance with amplitude  $A$ , shapes along proton and heteronuclear dimensions given by  $F_1$  and  $F_2$ , and a relaxation decay given by  $F_3$  (Figure 1). The components may be extracted from the experimental data by a least square fit of the model given by Equation 1. The model consists of  $N \cdot (I+J+K-2)$  adjustable parameters corresponding to the normalized shapes  $F_1$ ,  $F_2$  and  $F_3$ , and the amplitude for each of the  $N$  components. The quality of the least square fit is characterized by a loss function defined as the norm of the matrix of residuals (sum of squares of the elements  $e_{i,j,k}$ ). Details

of the computational procedure used in MUNIN and a brief survey of the literature on three-way decomposition can be found in (Orekhov et al., 2001). The main advantage of the model defined by Equation 1 stems from the fact that spectral components can be unambiguously resolved without any assumptions on the shapes  $F_1$ ,  $F_2$  and  $F_3$ . The only requirement is uniqueness of the shapes in all three dimensions. A special case referred in the following as ‘mixing’ accrues if two or more components have identical shapes in one of the dimensions. The solution for these components is not unique with respect to arbitrary linear combinations between them.

#### *MUNIN versus ordinary analysis*

To check the robustness of the method, MUNIN calculations were performed for 117 isolated resonances found in the  $^1\text{H}$ - $^{15}\text{N}$  correlation spectra of azurin. Small spectral regions comprising each one peak were selected. For each region, MUNIN calculations assuming a single component (i.e., choosing  $N = 1$  in Equation 1) were performed on the three-dimensional arrays formed by the 11 two-dimensional spectra comprising the  $^{15}\text{N}$   $R_{1\rho}$  data for each offset of the spin-lock carrier frequency. The  $^{15}\text{N}$   $R_{1\rho}$  values were then extracted by a two-parametric exponential fit on the shape along the ‘relaxation’ dimension. The  $R_{1\rho}$  values calculated in this way were compared with those obtained from the decays of peak maxima in the two-dimensional spectra (the latter is henceforth referred to as ‘ordinary analysis’). This test on MUNIN was performed for all 19 spin-lock offsets on 117 isolated resonances, providing a statistical basis of 2223 comparisons.

The results of the comparison are shown in Figure 2. The distribution of normalized deviations between the MUNIN results and those from ordinary analysis is symmetric and centered at zero, indicating the absence of any systematic differences between the relaxation rates obtained by the two methods. The width of the distribution is even narrower than expected if the results of both procedures would be uncorrelated, confirming the high coincidence within the anticipated uncertainties of the results from MUNIN and the ordinary analysis. Both procedures result in uncertainties of the relaxation rates ranging from 1% to 4% depending on the spin-lock offset. MUNIN ‘relaxation’ shapes provide a slightly better exponential fitting than those obtained using directly spectral peak maxima (data not shown). This is probably due to the

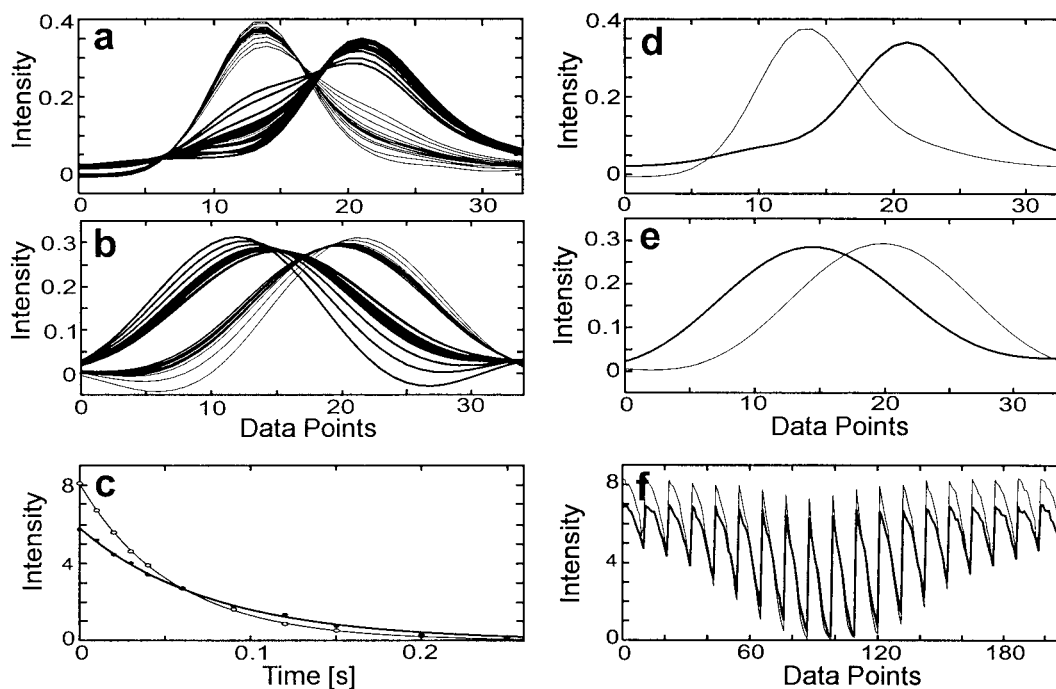


**Figure 1.** Shapes along the  $^1\text{H}$  (a, d),  $^{15}\text{N}$  (b, e) and ‘relaxation’ (c, f) dimensions for two components obtained from three-way decomposition and corresponding to the overlapped NH resonances of S4 and M13 of azurin. (a, b) Decompositions of three-dimensional arrays each formed by 11 two-dimensional spectra for 18 different spin-lock offsets from the carrier of the  $^{15}\text{N}$  pulses. On the plot c the ‘relaxation’ shapes for the two components are presented versus spin-lock length for the set with zero spin-lock offset from the carrier of the  $^{15}\text{N}$  pulses. The lines in c show the exponents providing best fits for the corresponding shapes. (d, e, f) Decomposition of the three-dimensional array formed by all 209  $R_{1\rho}$  spectra. On the plot f the 209 points in ‘relaxation’ shape describe all 19 relaxation decays (11 points each) recorded with different spin-lock offsets. The  $^1\text{H}$  and  $^{15}\text{N}$  shapes are normalized whereas the ‘relaxation’ shapes contain the amplitudes of the components. One point in the  $^1\text{H}$  and  $^{15}\text{N}$  dimension corresponds to 2.5 Hz and 1.5 Hz, respectively. Note that amplitudes in the relaxation decays are affected by relaxation during adiabatic pulses.

fact that MUNIN utilizes the decay of the entire peak region and partially filters out the noise.

#### *MUNIN applied to overlapped resonances*

The only example of strongly overlapped NH resonances from different residues in the  $^1\text{H}$ - $^{15}\text{N}$  spectrum of azurin is the region containing the peaks from S4 and M13, which are separated by 18 Hz in the  $^1\text{H}$  and 8 Hz in the  $^{15}\text{N}$  dimension (Figure 3a). For each of the 19 offsets of the  $^{15}\text{N}$  spin-lock carrier frequency the three-dimensional arrays composed of the region containing the S4/M13 peaks in 11 two-dimensional spectra were analyzed with MUNIN and assuming two components ( $N = 2$  in Equation 1). The results of these analyses are shown in Figure 1a–c and Figure 3a. The resonances from S4 and M13 are separated due to their different relaxation behavior for 18 of the 19 spin-lock offsets. Similar  $^1\text{H}$  and  $^{15}\text{N}$  shapes for the two resulting components are obtained for the differ-

ent offsets (Figures 1a and 1b), confirming the validity of the separation achieved. In spite of the variations of the shapes visible within the bundles of curves representing the two components (Figures 1a and 1b), it will be shown below that precise  $R_{1\rho}$  values for all spin-lock offsets are obtained nonetheless. The two components for the largest negative offset ( $-7000$ ) are mixed due to the near identity of the relaxation data obtained for both residues (data not shown in Figure 1). Note that the demonstration of very similar relaxation rates for two peaks provides the requested information without need for proper peak separation, i.e., precise relaxation values are obtained also for this offset for both components. The exponential fits of the ‘relaxation’ dimensions (Figure 1c) yield values that provide offset dependencies of  $^{15}\text{N}$   $R_{1\rho}$  for the components (Figure 3a, filled squares and circles) that very well match the theoretical dependence (Peng et al., 1991). The observed difference in  $^{15}\text{N}$   $R_{1\rho}$  of S4 and M13 is in agreement with different mobility of

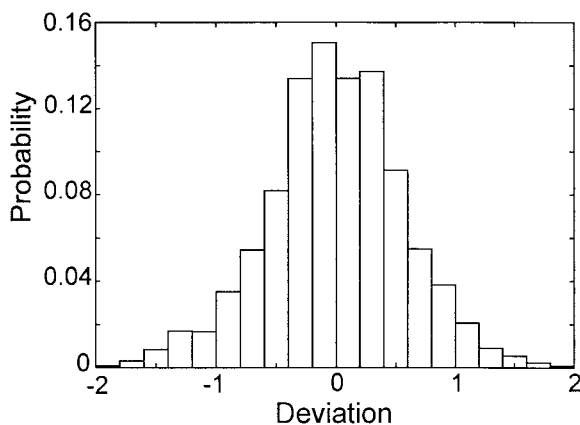


Figure 2. Distribution of normalized deviations,  $(^M R_{1\rho} - ^O R_{1\rho}) / (\Delta^O R_{1\rho}^2 + \Delta^M R_{1\rho}^2)^{1/2}$ , between  $^M R_{1\rho}$  resulting from MUNIN calculations and  $^O R_{1\rho}$  obtained from ordinary analysis for 117 isolated NH resonances of azurin.  $^M R_{1\rho}$ ,  $^O R_{1\rho}$  and their uncertainties  $\Delta^O R_{1\rho}$ ,  $\Delta^M R_{1\rho}$  were estimated by two-parametric exponential fitting of 'relaxation' shapes and decays of peak maxima, respectively. For each resonance MUNIN calculations were performed for 19 three-dimensional arrays composed of 11 two-dimensional spectra. Thus, the distribution was calculated based on 2223 pairs of  $R_{1\rho}$  values.

the corresponding protein regions revealed in a study of backbone dynamics (our preliminary data).

#### Analysis of large data sets

Although very similar, the  $^1\text{H}$  and  $^{15}\text{N}$  shapes of the two components representing S4 and M13 slightly differ for different spin-lock offsets (Figure 1a and 1b). Also, for one of 19 spin-lock offsets ( $-7000$  Hz from the carrier of  $^{15}\text{N}$  pulses) the  $^{15}\text{N}$   $R_{1\rho}$  values for S4 and M13 coincide, resulting in the same 'relaxation' shapes and non-unique  $^1\text{H}$  and  $^{15}\text{N}$  shapes due to mixing of the two components. The combined processing of the data obtained for different spin-lock offsets allows one to utilize the information about the  $^1\text{H}$  and  $^{15}\text{N}$  line-shapes from all two-dimensional spectra comprising  $R_{1\rho}$  data set. Such a processing provides the means for removing imperfections such as non-ideal or mixed shapes for particular offsets. The results of MUNIN processing of the three-dimensional array formed by the S4/M13 region from all 209  $^1\text{H}$ - $^{15}\text{N}$   $R_{1\rho}$  spectra (11 spectra for each of the 19 spin-lock offsets) are shown on Figure 1d–f. Although for several offsets the  $^1\text{H}$  and  $^{15}\text{N}$  shapes of the components differ from those obtained using smaller data sets comprising only 11 spectra (Figure 1), the fitted values of  $^{15}\text{N}$   $R_{1\rho}$  change very little (Figure 3a, open vs. filled squares and circles).

A more demanding example, illustrating the efficiency of the combined processing of data at multiple spin-lock offsets, is the group of three overlapped peaks presumably representing L68 NH (Figure 3b). Two of three overlapped peaks possess very similar relaxation rates at most spin-lock offsets, resulting in mixing for the corresponding components if the data are processed separately for each offset. Based on the complete three-dimensional data set for this region composed of all 209  $^1\text{H}$ - $^{15}\text{N}$  spectra, the three peaks are well separated by MUNIN, and  $^{15}\text{N}$   $R_{1\rho}$  values matching the theoretical dependence on the spin-lock offset are obtained for the three peaks.

#### Selection of the number of components

A common problem in analysis of crowded spectral regions is that the number of overlapped resonances may not be known *a priori*. With MUNIN this question can be addressed by performing calculations with a varying number of components. The selection of the appropriate number of components is then based on comparisons of the loss functions obtained in different calculations and the information provided by the additional components. In MUNIN calculations for the S4/M13 region (Figure 3a) based on all 209  $R_{1\rho}$  spectra the two-component model results in a reduction of the loss function by a factor of 5 if compared with the one-component model. Addition of a third component provides only 15% improvement of the data fit and does not affect the first two components. The third component has low amplitude and merely describes noise, indicating an adequate description of the data by two components. In calculations for the L68 region (Figure 3b) the loss function drops 3 times upon transition from the one- to the two-component model and then 2 times when adding a third component. Although the use of a four-component model further improves the fit, two of the four components have almost identical shapes in the first two dimensions and therefore describe the same peak (Orekhov et al., 2001), confirming that the data for L68 are adequately described by three components.

The two examples considered here represent difficult cases of spectral overlap in  $^1\text{H}$ - $^{15}\text{N}$  correlation spectra of 14 kDa azurin, which would escape quantitative analysis by ordinary methods. A systematic study exploring the borders of applicability and limitations of MUNIN requires extensive numerical simulations accounting for a number of factors such as signal to noise ratios, character of spectral noise, signal sep-

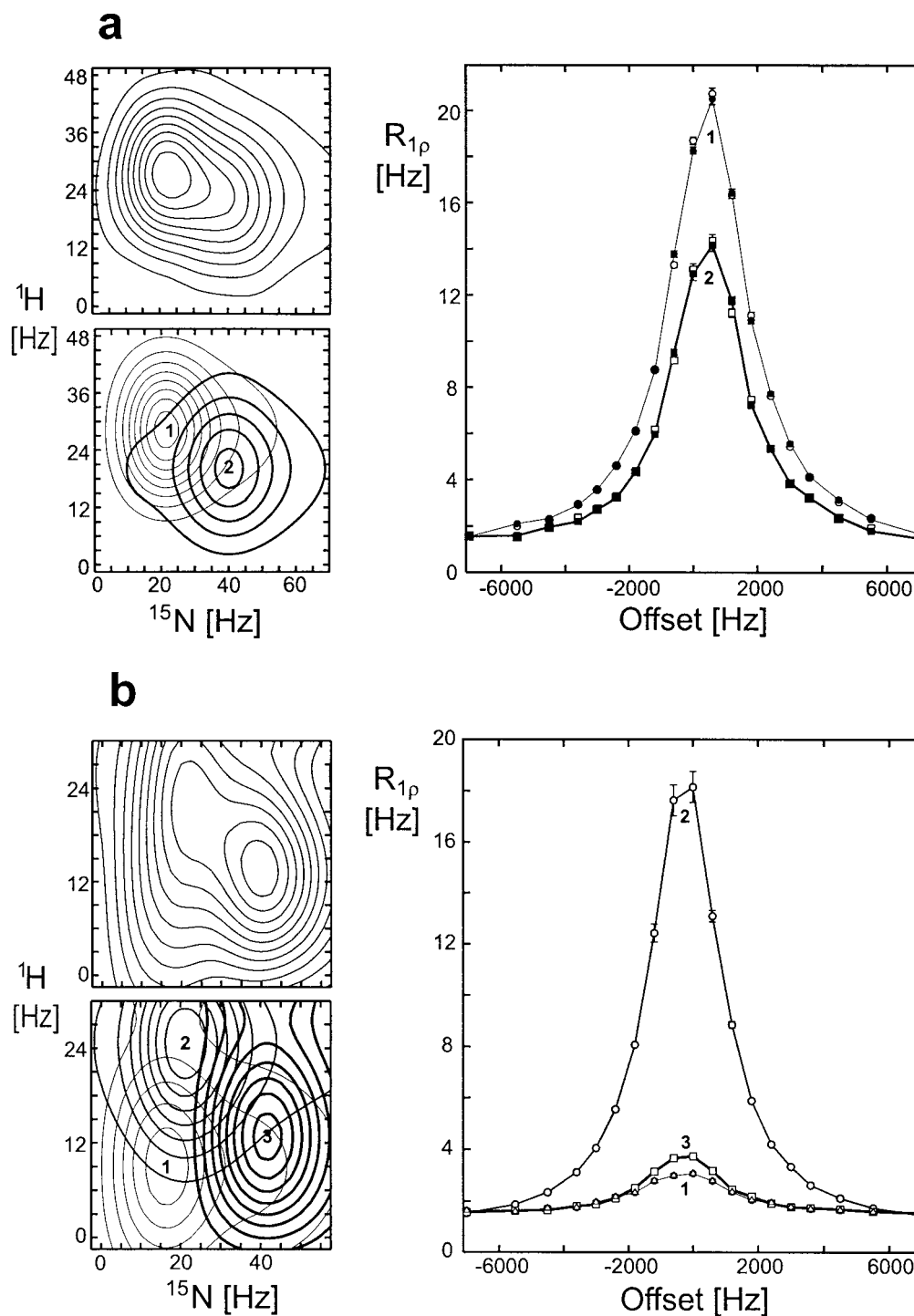


Figure 3. MUNIN decompositions of selected regions from  $^{15}\text{N}$   $R_{1\rho}$  spectra of azurin: (a) NH resonances from S4 and M13, (b) group of peaks around L68. For each example, the contour plots (drawn with equal spacing) represent the two-dimensional spectrum recorded with zero spin-lock offset from the carrier of  $^{15}\text{N}$  pulses at minimal spin-lock length (top) and its decompositions into components (bottom). Also shown are the dependencies of  $^{15}\text{N}$   $R_{1\rho}$  on the spin-lock offset from the carrier of the  $^{15}\text{N}$  pulses for all components. The  $R_{1\rho}$  values resulting from separate MUNIN analyses for different spin-lock offsets are shown by filled signs. Open signs denote the  $R_{1\rho}$  values obtained from combined MUNIN processing of all 209 two-dimensional spectra. The values of  $R_{1\rho}$  were calculated by two-parametric exponential fitting of the decays obtained from the 'relaxation' shapes.

arations, relative peak intensities, which is beyond the scope of the present communication.

In conclusion, three-way decomposition was applied to separate strongly overlapped resonances in a set of two-dimensional spectra modulated by relaxation. The major improvement of the resulting relaxation data lies in the possibility to obtain quantitative measurements for resonances that cannot be analyzed by traditional methods. The  $^{15}\text{N}$   $R_{1\rho}$  data at multiple offsets of the spin-lock carrier provide a specific example of the combined MUNIN processing of different sets of relaxation data. However, in complete analogy with this example any  $^1\text{H}$ - $^{15}\text{N}$ ( $^{13}\text{C}$ ) correlation based relaxation data (e.g.,  $^{15}\text{N}$ ( $^{13}\text{C}$ )  $R_1$ ,  $R_2$  and NOE's) may be combined for joint processing provided that they use identical schemes for recording the  $^{15}\text{N}$ ( $^{13}\text{C}$ )/ $^1\text{H}$  chemical shifts. MUNIN has also the potential to resolve overlap in complex regions of two-dimensional spectra by adding relaxation or another modulation (e.g., from J-coupling or diffusion) as a third dimension. The potential to make use of a large variety of modulations in one or several dimensions opens a wide variety of future applications of MUNIN.

#### Acknowledgements

This work was supported by NFR grant K-AA/KU 12071-302, RFBR grant 00-04-48318 and a post-

doctoral fellowship from the Wenner-Gren Foundation to D.M.K. All NMR experiments were performed at the Swedish NMR Centre. The authors are grateful to Prof. A.S. Arseniev for helpful discussion and to Dr G. Karlsson for providing us with a uniformly  $^{15}\text{N}$  labeled sample of azurin.

#### References

- Bro, R. (1997) *Chemometrics Intell. Lab. Syst.*, **38**, 149–171.
- Caffrey, M., Kaufman, J., Stahl, S.J., Wingfield, P.T., M., G.A. and Clore, G.M. (1998) *J. Magn. Reson.*, **135**, 368–372.
- Karlsson, B.G., Pascher, T., Nordling, M., Arvidsson, R.H.A. and Lundberg, L.G. (1989) *FEBS Lett.*, **246**, 211–217.
- Kay, L.E. (1998) *Nat. Struct. Biol.*, **5**, 513–517.
- Korzhev, D.M., Billeter, M., Arseniev, A.S. and Orekhov, V.Y. (2001) *Prog. Nucl. Magn. Reson. Spectrosc.*, **38**, 197–266.
- Kumar, A., Grace, R.C.R. and Madhu, P.K. (2000) *Prog. Nucl. Magn. Reson. Spectrosc.*, **37**, 191–319.
- Mulder, F.A.A., de Graaf, R.A., Kaptein, R. and Boelens, R. (1998) *J. Magn. Reson.*, **131**, 351–357.
- Orekhov, V.Y., Ibraghimov, I. and Billeter, M. (2001) *J. Biomol. NMR*, **20**, 49–60.
- Palmer, A.G., Williams, J. and McDermott, A. (1996) *J. Phys. Chem.*, **100**, 13293–13310.
- Peng, J.W., Thanabal, V. and Wagner, G. (1991) *J. Magn. Reson.*, **94**, 82–100.